

Fast Preemption: Forward-Backward Cascade Learning for Efficient and Transferable Proactive Adversarial Defense

Hanrui Wang¹, Ching-Chun Chang¹, Chun-Shien Lu², Isao Echizen¹

¹National Institute of Informatics (NII); ²Academia Sinica

¹Tokyo, Japan; ²Taipei, Taiwan

¹{hanrui_wang, ccchang, iechizen}@nii.ac.jp; ²lcs@iis.sinica.edu.tw

Abstract

Deep learning technology has brought convenience and advanced developments but has become untrustworthy due to its sensitivity to adversarial attacks. Attackers may utilize this sensitivity to manipulate predictions. To defend against such attacks, existing anti-adversarial methods typically counteract adversarial perturbations post-attack, while we have devised a proactive strategy that preempts by safeguarding media upfront, effectively neutralizing potential adversarial effects before the third-party attacks occur. This strategy, dubbed *Fast Preemption*, provides an efficient transferable preemptive defense by using different models for labeling inputs and learning crucial features. A forward-backward cascade learning algorithm is used to compute protective perturbations, starting with forward propagation optimization to achieve rapid convergence, followed by iterative backward propagation learning to alleviate overfitting. This strategy offers state-of-the-art transferability and protection across various systems. With the running of only three steps, our *Fast Preemption* framework outperforms benchmark training-time, test-time, and preemptive adversarial defenses. We have also devised the first, to our knowledge, effective white-box adaptive reversion attack and demonstrate that the protection added by our defense strategy is irreversible unless the backbone model, algorithm, and settings are fully compromised. This work provides a new direction to developing proactive defenses against adversarial attacks.

1. Introduction

Deep learning technologies have been demonstrated to be sensitive to adversarial attacks [18]. An adversarial attacker can utilize this weakness to manipulate medias such as images, audios, and videos. For example, the attacker can change the identity of a face image to that of the attacker without changing the looking, enabling the attacker to il-

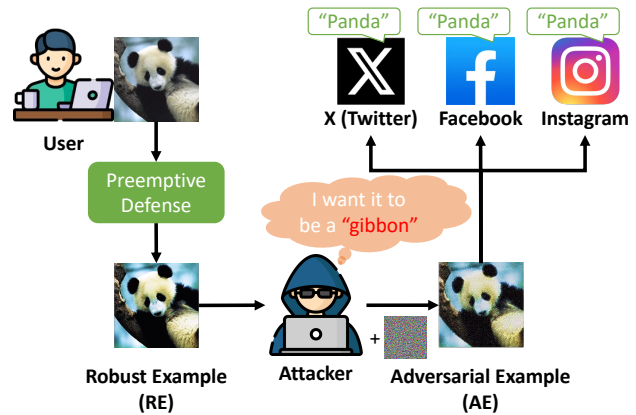


Figure 1. A preemptive defense offers transferable protection against an adversarial attack by preemptively manipulating the image before it is attacked.

legally access the face authentication system [47]. The attacker can also add slight noise on traffic signs, possibly causing an accident during autonomous driving [15]. Defending against such attacks is a critical but unsolved challenge. Passive defenses [6, 22, 29, 34], on the one hand, trade off classification accuracy for resistance against threats [54], but may be vulnerable to counterattacks [7, 46]. Proactive defenses [17, 32], on the other hand, do not achieve satisfactory time efficiency when running protection in real-time applications. Additionally, these proactive defenses typically require paired modules for protection and inference, so their protection is untransferable to other systems. Furthermore, if a provided model is used, the user may concern if backdoor exists in this model [39].

To address these problems, we devise a proactive strategy, called *Fast Preemption*, as illustrated in Fig. 1. *Fast Preemption* preemptively “attacks” (manipulates for enhancement) the medias from the user side before being attacked by the third party. Specifically, *Fast Preemption* learns robust features and predicts possible adversar-

ial perturbations, then enhances these robust features and reverses the predicted perturbations for purpose of protection. In this case, when these protected medias are further attacked, these adversarial perturbations will be automatically neutralized. This strategy has three distinct advantages. (i) A proactive preemptive defense provides better resistance against threats than a passive one without degrading accuracy, whereas Fast Preemption requires no additional operation for the classification system. (ii) Fast Preemption allows plug-and-play implementation because it does not require paired modules, alleviating the security and privacy concerns through a backdoor when using another provider’s system [16, 39]. (iii) From the attacker’s perspective, once a training- or test-time defense (typically integrated within a classification model) is breached, all inputs are affected. In contrast, with this preemptive defense, only a single user is affected as users are likely to be using different settings. Therefore, Fast Preemption meets four basic requirements:

- *Preserve clean accuracy and improve robust accuracy:* Basic requirements for all defenses.
- *Not require ground truths:* It is impractical to label each input manually.
- *Provide an efficient defense:* Time cost per process must be satisfactory for user interaction.
- *Be transferable to other systems:* Effect of protection must be transferable across various systems, so users do not have to use a paired module.

We propose the Fast Preemption defense includes three components: a classifier model for automatically labeling inputs, a backbone model for learning features (differ from the classifier), and the forward-backward (*Fore-Back*) cascade learning algorithm for efficiently computing transferable protective perturbations. We conducted evaluation on two datasets [2, 26] across six models [6, 13, 19, 29, 32, 35], defending against two typical adversarial attacks [11, 31]. The results demonstrate the superior performance of the Fast Preemption strategy in terms of clean and robust accuracies, transferability, and time cost compared with those of benchmark training-time, test-time, and preemptive adversarial defenses [6, 17, 29, 32, 34]. For example, in an end-to-end comparison with the state-of-the-art (SOTA) preemptive defense [32] on the ImageNet dataset [2], Fast Preemption attained 1.5% and 5.6% increases in terms of the clean and robust accuracies, respectively, against AutoAttack (Standard) [11] and was 33 times faster.

Shannon insightfully claimed that “One ought to design systems under the assumption that the enemy will immediately gain full familiarity with them [43].” On the basis of that assumption, Bi-Level [29] *first* proposed a reversion attack but failed, claiming their defense was irreversible. However, our reversion attack successfully defeated their defense, establishing ours as the *first effective* adaptive re-

version attack in the white-box setting, dubbed *Preemptive Reversion*, for evaluating the reliability of preemptive defenses, *i.e.*, whether they are reversible. Preemptive Reversion conducts the secondary preemptive defense upon the protected example and then reverses these new perturbations because, in the same setting, the secondary defense offers mostly the same perturbations as the first defense. Along with adaptive reversion, we propose using a more comprehensive evaluation protocol, one that requires a decrease in the clean accuracy after the instance is preemptively defended (which is ensured by selecting a poor classifier). If clean accuracy increases after reversion, the reversion succeeded. If it decreases after reversion (due to distortion), reversion failed.

The results from reversion attack testing demonstrate that the Preemptive Reversion attack can smartly erase protective perturbations when all defense details are compromised (*i.e.*, a white-box situation), whereas blind JPEG distortion and adversarial purification [34] only further distort an image. However, this white-box situation is impractical with the Fast Preemption strategy for real-world applications because the proposed framework enables users to individually customize their defense settings. Apart from a white-box situation, Fast Preemption protection cannot be reversed using existing reversion approaches.

We summarize our contributions as follows: (i) We present a new preemptive defense strategy (Fast Preemption) providing more transferable protection without requiring ground truths or requiring users to use a paired module. It is the first to use different models for the classifier and backbone. (ii) We present a forward-backward (*Fore-Back*) cascade learning algorithm that speeds up preemptive defense for efficient user interaction. (iii) We present the first effective adaptive reversion attack (*Preemptive Reversion*) for evaluating the reliability of preemptive defenses in a white-box setting and a more comprehensive protocol to evaluate whether reversion succeeds.

2. Related Work

Existing adversarial defenses can be categorized into three primary types: training-time, test-time, and preemptive defenses. Appendix A provides a more detailed review.

Training-time defenses produce robust deep learning models that may correctly classify adversarial examples (AEs) as their ground truth labels [6, 13, 14, 18, 19, 29, 35, 41, 42, 44, 50, 54]. However, they have two shortcomings. First, they require vast amounts of data for training, and the data quality and diversity are crucial to robustness. Second, training-time defenses typically reduce clean accuracy in favor of robust accuracy.

Test-time defenses are divided to detection and purification. Detection models are typically trained on AEs to enable the model to distinguish them from benign inputs

[9, 22, 27, 56]. However, detection of unseen attacks is challenging for all existing detectors because they are trained on AEs from known attacks. Additionally, detection always introduces errors due to false classification of benign images as AEs, thus reducing clean accuracy. In contrast, adversarial purification aims to purify AEs by eliminating or invalidating perturbations. Earlier studies used image distortion for purification [20, 37, 48]. Lately, more practical approaches generate benign replacements for inputs regardless of whether they are malicious [34, 38]. The major limitation of purification is that the difference between the original and generated examples degrades clean accuracy, and the possibility of being counterattacked [7, 46].

Preemptive defenses seek to generate robust examples (REs) that replace the original images, which are subsequently discarded [17, 32, 40]. These REs are inherently more difficult to manipulate, thereby providing resistance against adversarial attacks. However, such approaches face significant limitations, including high computational costs, limited transferability across models, and, in some cases, lower robustness compared to other defense mechanisms.

Lastly, Alfarra *et al.* [3] introduced a test-time defense mechanism incorporating preemptive defense as an anti-adversary layer guided by the output of a standard classifier. However, this defense can be circumvented if the classifier is compromised, a limitation explicitly acknowledged in their paper. This significant vulnerability undermines the practicality of using preemptive defense techniques in test-time scenarios. While they characterize this scenario as a “least realistic setting,” we contend that it aligns with the standard white-box attack paradigm, where adversaries have full access to the model. Under even more challenging assumptions, adversaries might also be aware of the defense mechanism itself (white-box reversion). Furthermore, the approach of Alfarra *et al.* [3] depends exclusively on forward propagation-based learning, which increases the risk of overfitting.

3. Preemptive Defense: Fast Preemption

With the preemptive defense strategy, the image is preemptively “attacked” (manipulated for enhancement), protecting it before being attacked. In this section, we present the framework and algorithm of our Fast Preemption strategy.

3.1. Problem Definition

Adversarial attacks and preemptive defenses both manipulate inputs by adding subtle perturbations. Specifically, let x and y denote the original image and its ground-truth label, respectively, and let f_v denote the victim model. Let x' denote the manipulated example (AE or RE), formulated as

$$x' = x + \delta, \text{ s.t. } \|\delta\|_p \leq \epsilon, \quad (1)$$

where δ denotes the perturbations, $\|\cdot\|_p$ represents the L_2 - or L_∞ -norm and ϵ is the setting of the maximum distance. Therefore, adversarial attacks and preemptive defenses aim to solve different optimization problems (as explained below) by changing δ with the inputs of x , y , and f_v .

3.1.1 Adversarial Attack

An adversarial attack leads to misclassification due to subtle perturbations. Given an original image x and its ground truth y , the adversarial attacker is able to generate an AE by maximizing the cross entropy (CE) loss of x for label y , thereby reducing the model’s confidence in correctly classifying the input as its true label. Therefore, the optimization objective of an adversarial attack for misclassification is

$$\arg \max_{\delta} CE(f_v(x + \delta), y). \quad (2)$$

3.1.2 Preemptive Defense

A preemptive defense aims to generate REs those will make Eq. (2) less successful. With the preemptive defense strategy, “backward propagation optimization” is used to reverse the adversarial attack perturbations [32]. In other words, the optimization of Eq. (2) remains, but output δ is reversed. The backward propagation optimization is formulated as

$$\arg \max_{\delta} CE(f_v(x - \delta), y). \quad (3)$$

In contrast to backward propagation optimization, we newly define “forward propagation optimization” for the preemptive defense strategy. It directly reverses the optimization direction of Eq. (2) from maximization to minimization, which in turn enhances the model’s confidence in accurately classifying the input according to its true label:

$$\arg \min_{\delta} CE(f_v(x + \delta), y). \quad (4)$$

3.2. Framework

As illustrated in Fig. 2, the Fast Preemption framework includes three components.

Classifier: Correct input labels determines the correct optimization direction for defense. However, for efficient user interaction, it is impractical to label each input manually. Classifier f_c labels these inputs automatically. Therefore, y in Eq. (3) and Eq. (4) can be replaced by $f_c(x)$. The framework is integrated with user application before being attacked, so f_c does not have to show any transferability or resistance against threats, but it must offer the best classification accuracy. Processing images with ground truths can be regarded as using a perfect classifier.

Backbone Model: With Fast Preemption, the input image is iteratively optimized on backbone model f_b , which

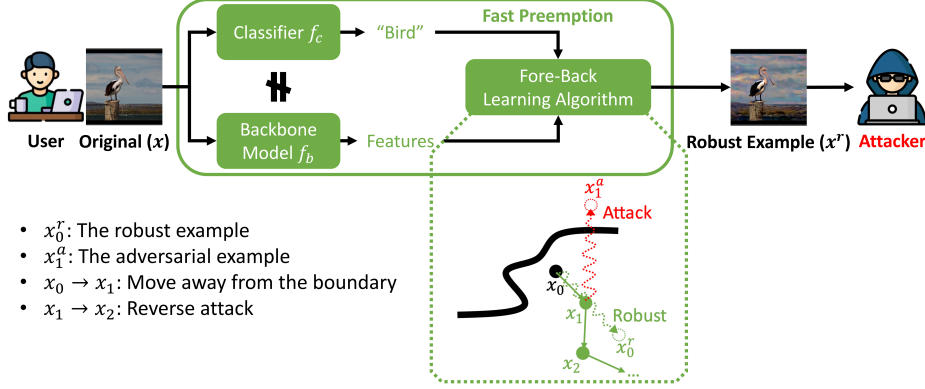


Figure 2. Fast Preemption framework. The classifier labels inputs automatically, which improves clean accuracy and thereby improves defense performance. The backbone model learns crucial features, so it must be adversarially trained. The Fore-Back learning algorithm first runs forward propagation ($x_0 \rightarrow x_1$) to quickly move away from the incorrect classes and then runs backward propagation ($x_1 \rightarrow x_2$) to alleviate overfitting on the backbone model.

may differ from victim model f_v in Eq. (3) and Eq. (4). Therefore, due to its complexity, f_b determines the transferable clean and robust accuracies and time cost. To achieve better performance, the backbone model f_b must be adversarially trained so it can learn more crucial features instead of random pixels. The limitations of adversarially trained models (*i.e.*, training-time defenses), such as the degradation of clean accuracy, are alleviated by the well-performing nonrobust classifier f_c in our framework. As a result, the preemptive defense optimizes the inputs towards the correct labels. Therefore, two different models, classifier f_c and backbone f_b , are integrated into the framework.

Fore-Back Cascade Learning Algorithm: To meet our framework, the optimization problems formulated as Eq. (3) and Eq. (4) can be reformulated as

$$\arg \max_{\delta} CE(f_b(x - \delta), f_c(x)), \quad (5)$$

$$\arg \min_{\delta} CE(f_b(x + \delta), f_c(x)), \quad (6)$$

respectively, where f_c is our classifier and f_b is our backbone model. This cascade learning algorithm is described in detail in the next section.

3.3. Forward-Backward Cascade Learning

The Fore-Back cascade learning algorithm is used to compute protective perturbations. The input is first moved away from the classification boundaries of all incorrect classes so that the manipulated input will be easier to be classified as the ground truth. We define this as *forward propagation* (\rightarrow). Forward propagation can quickly attain convergence (less time cost) but causes overfitting on the backbone model so that the defense is less transferable to other victim models. *Backward propagation* optimization (\leftarrow) is thus conducted following forward propagation. Backward propagation reverses the adversarial perturbations to make them

protective perturbations, which effectively alleviates overfitting and thereby improves transferability. In summary, the forward and backward propagation both enhance robustness, but in different optimization directions. The complete algorithm is presented in Algorithm 1 of Appendix B.

3.3.1 Loss Function

From Eq. (5) and Eq. (6), the loss function of our Fore-Back cascade learning algorithm is the CE loss:

$$\ell(x_i|x, f_c, f_b) = CE(f_b(x_i), f_c(x)), \quad (7)$$

where x_i and x denote the output example of the i -th iteration and the original input, respectively, and f_c and f_b are our classifier and backbone models, respectively. The forward optimization reduces ℓ , while the backward optimization increases it.

3.3.2 Preliminary - Backward Propagation

The use of backward propagation for preemptive defense was introduced in the SOTA preemptive defense strategy [32]. At each step of that strategy, a projected gradient descent (PGD) attack [31] is run first as $x_1 \rightarrow x_1^a$ (Fig. 2), and then the adversarial perturbations are reversed in accordance with the learning rate and thereby forms protective perturbations, as $x_1 \rightarrow x_2$.

Specifically, backward propagation first runs an I -iteration L_∞ -norm PGD attack from x_t , which is the output of the previous optimization step (forward or backward). In other words, the backward propagation increases ℓ via

$$\begin{aligned} x_{t,0} &= x_t, \\ x_{t,i+1} &= \prod_{x,\epsilon} (x_{t,i} + \alpha \cdot \text{sign}(\nabla \ell(x_{t,i}|x, f_c, f_b))), \quad (8) \\ \text{s.t. } & \|x_{t,i+1} - x\|_\infty \leq \epsilon \ \& \ 0 \leq i < I - 1, \end{aligned}$$

where ϵ is the setting of the maximum distance and α is the step size. The final output of Eq. (8) is AE x_t^α . Next, backward propagation subtracts perturbations $x_t^\alpha - x_t$ from x_t in accordance with learning rate η , thereby computing the next robust example, x_{t+1} :

$$\begin{aligned} x_{t+1} &= \prod_{x,\epsilon} (x_t - \eta \cdot (x_t^\alpha - x_t)) \\ &= \prod_{x,\epsilon} (x_t - \eta \cdot \alpha \cdot \sum_{i=1}^I \text{sign}(\nabla \ell(x_{t,i}|x, f_c, f_b))). \end{aligned} \quad (9)$$

The SOTA preemptive defense strategy [32] conducts only backward propagation learning. However, adversarial attacks can be randomly initialized, so backward propagation requires many steps to converge (minimum ten steps). The Fast Preemption strategy accelerates defense by running forward propagation before running backward propagation learning.

3.3.3 Combining Forward and Backward Propagation

We define forward propagation learning as a direct enhancement by moving away from the decision boundary in accordance with the learning rate ($x_0 \rightarrow x_1$ in Fig. 2). Therefore, it first reduces ℓ via

$$\begin{aligned} x_{t,0} &= x_t, \\ x_{t,i+1} &= \prod_{x,\epsilon} (x_{t,i} - \alpha \cdot \text{sign}(\nabla \ell(x_{t,i}|x, f_c, f_b))), \quad (10) \\ \text{s.t. } & \|x_{t,i+1} - x\|_\infty \leq \epsilon \ \& \ 0 \leq i < I - 1, \end{aligned}$$

the final output of which is robust example x_t^r . Subsequently, protective perturbations $x_t^r - x_t$ are directly added to x_t in accordance with learning rate η :

$$\begin{aligned} x_{t+1} &= \prod_{x,\epsilon} (x_t + \eta \cdot (x_t^r - x_t)) \\ &= \prod_{x,\epsilon} (x_t - \eta \cdot \alpha \cdot \sum_{i=1}^I \text{sign}(\nabla \ell(x_{t,i}|x, f_c, f_b))), \end{aligned} \quad (11)$$

which is the same as for Eq. (9). Therefore, the above derivations can be summarized as

$$\begin{aligned} x_{t,0} &= x_t, \\ x_{t,i+1} &= \begin{cases} \prod_{x,\epsilon} (x_{t,i} - \alpha \cdot \text{sign}(\nabla \ell(x_{t,i}|x, f_c, f_b))) & \rightarrow \\ \prod_{x,\epsilon} (x_{t,i} + \alpha \cdot \text{sign}(\nabla \ell(x_{t,i}|x, f_c, f_b))) & \leftarrow \end{cases} \\ x_{t+1} &= \prod_{x,\epsilon} (x_t - \eta \cdot \alpha \cdot \sum_{i=1}^I \text{sign}(\nabla \ell(x_{t,i}|x, f_c, f_b))), \\ \text{s.t. } & \|x_* - x\|_\infty \leq \epsilon \ \& \ 0 \leq i < I - 1, \end{aligned} \quad (12)$$

where x_* denotes $x_{t,i+1}$ or x_{t+1} . Equation (12) indicates that both forward and backward propagation make inputs more robust but with different learning directions for loss ℓ .

Whereas backward propagation requires many steps to converge, forward propagation converges quickly. However, forward propagation causes overfitting of the backbone model, so the defense will be less transferable to other victim models. Fast Preemption alleviates this overfitting: T_{\rightarrow} steps of forward propagation are run until there is slight overfitting; then T_{\leftarrow} steps of backward propagation are run to eliminate the overfitting. We evaluated whether the learning is overfitted by evaluating transferability. With this combination of forward and backward propagation, Fast Preemption attains SOTA performance with only three steps (one step T_{\rightarrow} , followed by two steps T_{\leftarrow}), which dramatically reduces the time cost of RE generation.

3.3.4 Averaging N Examples

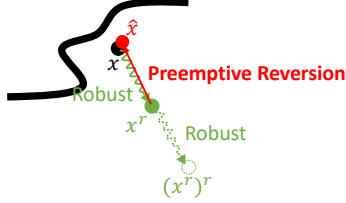
Forward and backward propagation both require a backbone optimization algorithm, *i.e.*, an adversarial attack algorithm. For example, The Bi-Level optimization [32] used PGD [31] for backward propagation. However, PGD has to run many sequential iterations to compute superior adversarial perturbations, which greatly increases the time cost. With the Fast Preemption strategy, Fast Gradient Sign Method (FGSM) [18] is used to speed up the computation of adversarial perturbations.

Since FGSM has difficulty obtaining optimal perturbations, with the Fast Preemption strategy, it is run N times with random initialization to produce N FGSM examples. The perturbations are then averaged to obtain the final output. We demonstrate that averaging the perturbations for PGD examples negligibly affects performance, whereas with the Fast Preemption strategy, FGSM optimization is effectively improved while efficiency is preserved.

Furthermore, averaging perturbations in the N FGSM examples is faster than processing a single example with iterative PGD. To generate a single RE, iterative PGD has to run each iteration sequentially from a single input, whereas N FGSM examples can be produced by repeating the single input N times and processing the results in parallel.

4. Adaptive Attack: Preemptive Reversion

A reversion attack is used to evaluate whether a preemptive defense is reversible. While Bi-Level [32] *first* proposed a reversion attack but failed, claiming their defense was irreversible, our reversion attack successfully defeated their defense, establishing ours as the *first effective* reversion attack. In this section, we present the algorithm for our proposed Preemptive Reversion and a more comprehensive protocol for evaluating the effectiveness of reversion attacks. Preemptive Reversion is the only feasible approach to reverse



- $x \rightarrow x^r$: Preemptive defense
- $x^r \rightarrow (x^r)^r$: Preemptive defense in same setting
- $\tilde{x} = x^r - ((x^r)^r - x^r)$: Assume preemptive defenses manipulating similar pixels

Figure 3. Illustration of Preemptive Reversion algorithm. It first conducts a secondary preemptive defense on RE x^r and then reverses the perturbations of the secondary defense: $(x^r)^r - x^r$.

preemptive defense in the white-box scenario. Nevertheless, without full knowledge of the backbone model and settings, our Fast Preemption defense is hard to reverse, so it is reliable.

4.1. Algorithm

When running preemptive defenses sequentially for the same input and settings, the perturbations are mostly the same for two rounds (see Fig. 5). On the basis of this finding, we devised the first effective white-box adaptive reversion attack, *i.e.*, *Preemptive Reversion*, as illustrated in Fig. 3. The complete algorithm is presented in Algorithm 2 of Appendix B. Using RE x^r generated by a preemptive defense method, the Preemptive Reversion algorithm first runs a secondary preemptive defense upon x^r to obtain $(x^r)^r$. Then, the Preemptive Reversion algorithm reverses the secondary perturbations from x^r to obtain \tilde{x} , which is the prediction of the original input x :

$$\tilde{x} = x^r - ((x^r)^r - x^r). \quad (13)$$

4.2. Attack Scenarios

We define two scenarios for a reversion attack in accordance with the knowledge the attacker has about the backbone model and defense algorithm:

- *White-Box*: The attacker knows both the backbone model and defense algorithm (including settings), so the attacker can conduct a secondary defense the same as the user does. This is the strongest, yet impractical, assumption because different users may use different settings.
- *Black-Box*: The attacker knows the defense algorithm (typically public) but not the backbone model (infinite selections for users). The challenge for the attacker in this scenario is that the crucial features learned in the secondary defense may differ from those learned by the user. Our proposed Preemptive Reversion attack is the first effective reversion attack for evaluating the reversibility of pre-

emptive defenses, including our Fast Preemption defense, but it is feasible only in the white-box scenario. Without full knowledge of the defense, Fast Preemption is reliable.

4.3. Evaluation Protocol

If a reversion attack succeeds, the improved clean accuracy should drop. However, image distortion can create a similar effect. Consequently, a drop in clean accuracy does not necessarily indicate the success of a reversion attack. To address this issue, we proposed a comprehensive protocol that can distinguish successful reversion from distortion. First, we purposely give incorrect labels to partial inputs to guarantee that the clean accuracy after being defended is lower than the original accuracy. In this situation, if the clean accuracy approaches close to the original accuracy, the reversion attack succeeded. Otherwise, the reversion attack failed, and the deterioration was caused by distortion.

5. Experiments

5.1. Datasets, Classifier, and Backbone Models

We conducted experiments on two datasets: CIFAR-10 [26] and ImageNet [2]. For CIFAR-10, ResNeXt29-32x4d [21] and PreActResNet-18 [19] were selected as the classifier and backbone model, respectively. For ImageNet, DeiT Base [45] and ConvNeXt-L+ConvStem [44] were selected as the classifier and backbone model, respectively. The model architectures are listed in Tab. 4 of Appendix D.

5.2. Attacks and Defenses

Adversarial attacks. We evaluated defenses against two adversarial attacks: PGD [31] and AutoAttack [11]. For AutoAttack, we used both its “Standard” version (combining APGD-CE, APGD-DLR, and FAB [10] and Square Attack [4]) and its “Random” version (combining APGD-CE and APGD-DLR, with expectation over time (EOT) equal to 20 [5]). **Reversion attacks.** We ran reversion attacks to evaluate: (i) whether the protected samples induced by preemptive defenses cannot be easily and precisely reversed back to their original unprotected status, which we define as “irreversible” in this paper; (ii) whether the proposed adaptive reversion attack, Preemptive Reversion, is effective. Therefore, apart from the specific Preemptive Reversion, we also ran reversion attacks using blind distortion (JPEG compression) and adversarial purification (DiffPure [34]).

Training-time defenses: We compared Fast Preemption with WideResNet-94-16 [6] and Swin-L [29] on the CIFAR-10 and ImageNet datasets, respectively. The model architectures of these defenses differ from the backbone models. **Test-time defenses:** We used DiffPure [34] as the benchmark test-time defense. The inputs were purified by DiffPure and then fed into WideResNet-94-16 [6] or Swin-L [29] in accordance with the dataset used. **Preemptive**

Table 1. End-to-end performance against AutoAttack [11] and comparison with benchmark adversarial defenses.

Dataset	Defense	Time Cost (s)	Clean (%)	Standard L_∞ (%)	Standard L_2 (%)	Random L_∞ (%)	
CIFAR-10	Training-Time	WideResNet-94-16 [6]	0	93.4	74.6	69.6	74.8
	Test-Time	DiffPure [34]	0.3	91.4	78.1	84.9	78.4
	Preemptive	A^5 [17]	0.01	93.5	73.8	69.0	74.3
		Bi-Level [32]	28	92.5	81.4	78.6	81.6
		Fast Preemption (ours)	0.04	95.0	86.5	84.3	86.7
Fast Preemption (ours) + DiffPure [34]	0.34	94.2	89.1	92.8	89.7		
ImageNet	Training-Time	Swin-L [29]	0	93.0	67.0	59.5	67.5
	Test-Time	DiffPure [34]	1.2	88.8	73.7	79.4	73.8
	Preemptive	Bi-Level [32]	43	93.6	71.5	62.8	72.3
		Fast Preemption (ours)	1.3	95.1	77.1	67.4	78
		Fast Preemption (ours) + DiffPure [34]	2.5	93.3	82.9	87.6	83.4

Bold indicates the best performance.

Table 2. Preemptive defenses resist reversion attacks.

Original (%)	Classifier	Preemptive Defense		Clean (%)	Distortion JPEG (%)	Purification DiffPure (%)	Preemptive Reversion (ours)	
		Backbone	Approach				White (%)	Black (%)
93.5	Bi-Level	Bi-Level	Bi-Level	91.9	90.5	90.8	93.1	90.7
	Bi-Level	PreActResNet-18	Bi-Level	91.2	90.6	90.7	93.4	91.0
	Bi-Level	PreActResNet-18	Ours	91.3	90.5	90.5	93.4	90.6
	ResNeXt29-32x4d	PreActResNet-18	Ours	95.5	94.4	94.8	94.0	94.6

Numbers in red demonstrate that only our reversion attack is feasible but only in the white-box setting.

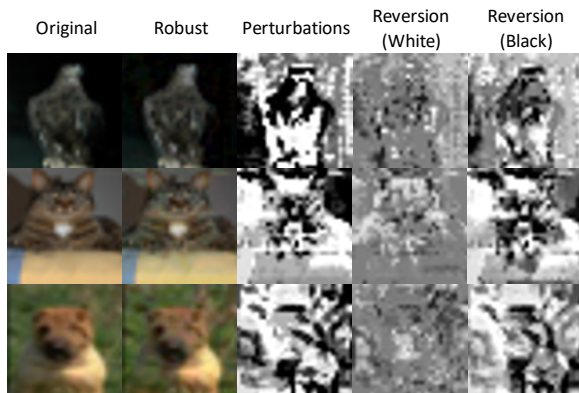


Figure 5. Perturbations before and after proposed Preemptive Reversion attack. White-box reversion successfully erased most protective perturbations while black-box reversion failed.

Reversion in the white-box setting was due to successful reversion, whereas the other decreases were due to distortion. Therefore, if only the results in the fourth row are considered, a decrease in accuracy does not necessarily indicate the effectiveness of a reversion attack.

7. Ablation Studies

We conducted ablation studies on the Fast Preemption framework and its learning algorithm using the CIFAR-10 dataset. We used AutoAttack (Standard) [11] against

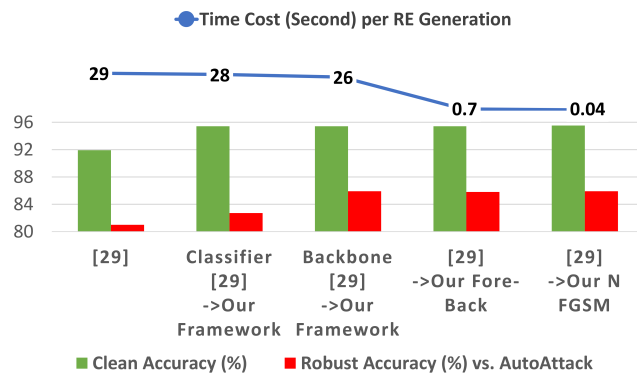


Figure 6. Compared with the SOTA preemptive defense Bi-Level [32], our framework improved the clean and robust accuracies, and our learning algorithm reduced the time cost for defense.

a black-box target model RaWideResNet-70-16 [35], employing L_∞ -norm perturbations with $\epsilon = 8/255$. As demonstrated in Fig. 6, Fast Preemption significantly outperforms the SOTA Bi-Level method [32], increasing clean accuracy from 92% to 95.3%, improving robust accuracy from 80.1% to 85.6%, and reducing computation time from 28 seconds to just 0.04 seconds. These studies were conducted to identify the optimal configurations, with more extensive ablation results presented in Appendix F.

8. Conclusion

We introduce an efficient and transferable preemptive adversarial defense, termed *Fast Preemption*. This approach establishes a novel layer in the defense hierarchy, Proactive Defense (ours) → Training-Time Defense → Test-Time Defense, distinct from conventional test-time and training-time defenses. The proposed mechanism is plug-and-play, transferable, and requires no prior knowledge, empowering users to safeguard media autonomously without reliance on third-party interventions. Moreover, our method addresses the efficiency limitations of proactive defenses, achieving processing speeds 700 times faster than existing approaches, a critical improvement for real-world applications where substantial delays (e.g., 28 seconds per image [32]) are infeasible. Finally, our approach maintains or enhances clean accuracy while delivering state-of-the-art robust accuracy, overcoming the common trade-off observed in other defense methods that degrade clean accuracy.

Nevertheless, our defense shows limitations against the proposed reversion attack in the white-box setting. While we design the defense allowing user customizing the backbone model (serving as a user-side key) to counter reversion attacks, simplifying user requirements is a priority for future work. Further research should also explore the relationship between backbone models and transferability, as discussed in Appendix F.2.

References

- [1] Sravanti Addepalli, Samyak Jain, et al. Efficient and effective augmentation strategy for adversarial training. *Advances in Neural Information Processing Systems (NIPS)*, 35:1488–1501, 2022. 6
- [2] Ian Goodfellow Alex K, Ben Hamner. Nips 2017: Defense against adversarial attack, 2017. 2, 6
- [3] Motasem Alfarra, Juan C Pérez, Ali Thabet, Adel Bibi, Philip HS Torr, and Bernard Ghanem. Combating adversaries with anti-adversaries. In *Proceedings of the AAAI Conference on Artificial Intelligence (AAAI)*, pages 5992–6000, 2022. 3, 2
- [4] Maksym Andriushchenko, Francesco Croce, Nicolas Flammarion, and Matthias Hein. Square attack: a query-efficient black-box adversarial attack via random search. In *European Conference on Computer Vision (ECCV)*, pages 484–501, 2020. 6, 5
- [5] Anish Athalye, Nicholas Carlini, and David Wagner. Obfuscated gradients give a false sense of security: Circumventing defenses to adversarial examples. In *International Conference on Machine Learning (ICML)*, pages 274–283, 2018. 6, 5
- [6] Brian R Bartoldson, James Diffenderfer, Konstantinos Parasyris, and Bhavya Kailkhura. Adversarial robustness limits via scaling-law and human-alignment studies. In *Forty-first International Conference on Machine Learning (ICML) Workshops*, 2024. 1, 2, 6, 7, 8, 3, 4, 5
- [7] Nicholas Carlini and David Wagner. Adversarial examples are not easily detected: Bypassing ten detection methods. In *Proceedings of the 10th ACM Workshop on Artificial Intelligence and Security (AISec)*, pages 3–14, 2017. 1, 3, 5, 7
- [8] Tianlong Chen, Sijia Liu, Shiyu Chang, Yu Cheng, Lisa Amini, and Zhangyang Wang. Adversarial robustness: From self-supervised pre-training to fine-tuning. In *Proceedings of the IEEE/CVF Conference on Computer Vision and Pattern Recognition (CVPR)*, pages 699–708, 2020. 6
- [9] Gilad Cohen, Guillermo Sapiro, and Raja Giryes. Detecting adversarial samples using influence functions and nearest neighbors. In *Proceedings of the IEEE/CVF Conference on Computer Vision and Pattern Recognition (CVPR)*, pages 14453–14462, 2020. 3, 1
- [10] Francesco Croce and Matthias Hein. Minimally distorted adversarial examples with a fast adaptive boundary attack. In *International Conference on Machine Learning (ICML)*, pages 2196–2205, 2020. 6, 5
- [11] Francesco Croce and Matthias Hein. Reliable evaluation of adversarial robustness with an ensemble of diverse parameter-free attacks. In *International Conference on Machine Learning (ICML)*, pages 2206–2216. PMLR, 2020. 2, 6, 7, 8, 3, 5
- [12] Francesco Croce, Maksym Andriushchenko, Vikash Sehswag, Edoardo Debenedetti, Nicolas Flammarion, Mung Chiang, Prateek Mittal, and Matthias Hein. Robustbench: a standardized adversarial robustness benchmark. In *Thirty-fifth Conference on Neural Information Processing Systems Datasets and Benchmarks Track (NeurIPS)*, 2021. 3, 5
- [13] Edoardo Debenedetti, Vikash Sehswag, and Prateek Mittal. A light recipe to train robust vision transformers. In *2023 IEEE Conference on Secure and Trustworthy Machine Learning (SaTML)*, pages 225–253, 2023. 2, 1, 3, 4, 6
- [14] Junhao Dong, Seyed-Mohsen Moosavi-Dezfooli, Jianhuang Lai, and Xiaohua Xie. The enemy of my enemy is my friend: Exploring inverse adversaries for improving adversarial training. In *Proceedings of the IEEE/CVF Conference on Computer Vision and Pattern Recognition (CVPR)*, pages 24678–24687, 2023. 2, 1
- [15] Kevin Eykholt, Ivan Evtimov, Earlene Fernandes, Bo Li, Amir Rahmati, Chaowei Xiao, Atul Prakash, Tadayoshi Kohno, and Dawn Song. Robust physical-world attacks on deep learning visual classification. In *Proceedings of the IEEE conference on computer vision and pattern recognition (CVPR)*, pages 1625–1634, 2018. 1
- [16] Matt Fredrikson, Somesh Jha, and Thomas Ristenpart. Model inversion attacks that exploit confidence information and basic countermeasures. In *Proceedings of the 22nd ACM SIGSAC conference on computer and communications security (ACM CCS)*, pages 1322–1333, 2015. 2
- [17] Iuri Frosio and Jan Kautz. The best defense is a good offense: Adversarial augmentation against adversarial attacks. In *Proceedings of the IEEE/CVF Conference on Computer Vision and Pattern Recognition (CVPR)*, pages 4067–4076, 2023. 1, 2, 3, 7, 8
- [18] Ian J Goodfellow, Jonathon Shlens, and Christian Szegedy. Explaining and harnessing adversarial examples. *arXiv preprint arXiv:1412.6572*, 2014. 1, 2, 5

- [19] Sven Gowal, Sylvestre-Alvise Rebuffi, Olivia Wiles, Florian Stimberg, Dan Andrei Calian, and Timothy A Mann. Improving robustness using generated data. In *Advances in Neural Information Processing Systems (NeurIPS)*, pages 4218–4233, 2021. [2](#), [6](#), [1](#), [3](#), [4](#), [5](#)
- [20] Chuan Guo, Mayank Rana, Moustapha Cisse, and Laurens van der Maaten. Countering adversarial images using input transformations. In *International Conference on Learning Representations (ICLR)*, 2018. [3](#), [1](#)
- [21] Dan Hendrycks, Norman Mu, Ekin Dogus Cubuk, Barret Zoph, Justin Gilmer, and Balaji Lakshminarayanan. Augmix: A simple data processing method to improve robustness and uncertainty. In *International Conference on Learning Representations (ICLR)*, 2019. [6](#), [3](#), [4](#), [5](#)
- [22] Thomas Hickling, Nabil Aouf, and Philippa Spencer. Robust adversarial attacks detection based on explainable deep reinforcement learning for uav guidance and planning. *IEEE Transactions on Intelligent Vehicles*, 2023. [1](#), [3](#)
- [23] Jonathan Ho, Ajay Jain, and Pieter Abbeel. Denoising diffusion probabilistic models. In *Proceedings of the 34th International Conference on Neural Information Processing Systems (NeurIPS)*, pages 6840–6851, 2020. [1](#), [2](#)
- [24] Tero Karras, Miika Aittala, Timo Aila, and Samuli Laine. Elucidating the design space of diffusion-based generative models. In *Advances in Neural Information Processing Systems (NeurIPS)*, pages 26565–26577, 2022. [1](#)
- [25] Diederik P Kingma and Max Welling. Auto-encoding variational bayes. In *International Conference on Learning Representations (ICLR)*, 2014. [2](#)
- [26] Alex Krizhevsky, Geoffrey Hinton, et al. Learning multiple layers of features from tiny images. Technical report, University of Toronto, 2009. [2](#), [6](#), [5](#)
- [27] Bin Liang, Hongcheng Li, Miaoqiang Su, Xirong Li, Wenchang Shi, and Xiaofeng Wang. Detecting adversarial image examples in deep neural networks with adaptive noise reduction. *IEEE Transactions on Dependable and Secure Computing*, 18(1):72–85, 2021. [3](#), [1](#)
- [28] Qinliang Lin, Cheng Luo, Zenghao Niu, Xilin He, Weicheng Xie, Yuanbo Hou, Linlin Shen, and Siyang Song. Boosting adversarial transferability across model genus by deformation-constrained warping. In *Proceedings of the AAAI Conference on Artificial Intelligence (AAAI)*, pages 3459–3467, 2024. [3](#), [5](#), [7](#)
- [29] Chang Liu, Yinpeng Dong, Wenzhao Xiang, Xiao Yang, Hang Su, Jun Zhu, Yuefeng Chen, Yuan He, Hui Xue, and Shibao Zheng. A comprehensive study on robustness of image classification models: Benchmarking and rethinking. *International Journal of Computer Vision*, pages 1–23, 2024. [1](#), [2](#), [6](#), [7](#), [8](#), [3](#), [5](#)
- [30] DC Livingston. Colorimetric analysis of the ntsc color television system. *Proceedings of the IRE*, 42(1):138–150, 1954. [7](#)
- [31] Aleksander Madry, Aleksandar Makelov, Ludwig Schmidt, Dimitris Tsipras, and Adrian Vladu. Towards deep learning models resistant to adversarial attacks. In *International Conference on Learning Representations (ICLR)*, 2018. [2](#), [4](#), [5](#), [6](#), [3](#)
- [32] Seungyong Moon, Gaon An, and Hyun Oh Song. Preemptive image robustification for protecting users against man-in-the-middle adversarial attacks. In *Proceedings of the AAAI Conference on Artificial Intelligence (AAAI)*, pages 7823–7830, 2022. [1](#), [2](#), [3](#), [4](#), [5](#), [7](#), [8](#), [9](#), [6](#)
- [33] Maria-Irina Nicolae, Mathieu Sinn, Minh Ngoc Tran, Beat Buesser, Amrisha Rawat, Martin Wistuba, Valentina Zantedeschi, Nathalie Baracaldo, Bryant Chen, Heiko Ludwig, Ian Molloy, and Ben Edwards. Adversarial robustness toolbox v1.2.0. *CoRR*, 2018. [3](#)
- [34] Weili Nie, Brandon Guo, Yujia Huang, Chaowei Xiao, Arash Vahdat, and Animashree Anandkumar. Diffusion models for adversarial purification. In *International Conference on Machine Learning (ICML)*, pages 16805–16827. PMLR, 2022. [1](#), [2](#), [3](#), [6](#), [8](#)
- [35] ShengYun Peng, Weilin Xu, Cory Cornelius, Matthew Hull, Kevin Li, Rahul Duggal, Mansi Phute, Jason Martin, and Duen Horng Chau. Robust principles: Architectural design principles for adversarially robust cnns. In *British Machine Vision Conference (BMVC)*, 2023. [2](#), [8](#), [1](#), [3](#), [4](#), [5](#), [6](#)
- [36] Rahul Rade and Seyed-Mohsen Moosavi-Dezfooli. Helper-based adversarial training: Reducing excessive margin to achieve a better accuracy vs. robustness trade-off. In *International Conference on Machine Learning (ICML) Workshop on Adversarial Machine Learning (AML)*, 2021. [6](#)
- [37] Edward Raff, Jared Sylvester, Steven Forsyth, and Mark McLean. Barrage of random transforms for adversarially robust defense. In *Proceedings of the IEEE/CVF Conference on Computer Vision and Pattern Recognition (CVPR)*, pages 6528–6537, 2019. [3](#), [1](#)
- [38] Min Ren, Yuhao Zhu, Yunlong Wang, and Zhenan Sun. Perturbation inactivation based adversarial defense for face recognition. *IEEE Transactions on Information Forensics and Security*, 17:2947–2962, 2022. [3](#), [2](#)
- [39] Aniruddha Saha, Akshayvarun Subramanya, and Hamed Pirsiavash. Hidden trigger backdoor attacks. In *Proceedings of the AAAI conference on artificial intelligence (AAAI)*, pages 11957–11965, 2020. [1](#), [2](#), [3](#)
- [40] Hadi Salman, Andrew Ilyas, Logan Engstrom, Sai Vemprala, Aleksander Madry, and Ashish Kapoor. Unadversarial examples: Designing objects for robust vision. In *Advances in Neural Information Processing Systems (NeurIPS)*, pages 15270–15284, 2021. [3](#), [2](#)
- [41] Vikash Schwag, Saeed Mahloujifar, Tinashe Handina, Sihui Dai, Chong Xiang, Mung Chiang, and Prateek Mittal. Robust learning meets generative models: Can proxy distributions improve adversarial robustness? In *International Conference on Learning Representations (ICLR)*, 2022. [2](#), [1](#), [6](#)
- [42] Ali Shafahi, Mahyar Najibi, Amin Ghiasi, Zheng Xu, John Dickerson, Christoph Studer, Larry S Davis, Gavin Taylor, and Tom Goldstein. Adversarial training for free! In *Proceedings of the 33rd International Conference on Neural Information Processing Systems (NeurIPS)*, pages 3358–3369, 2019. [2](#), [1](#)
- [43] Claude E Shannon. Communication theory of secrecy systems. *The Bell system technical journal*, 28(4):656–715, 1949. [2](#)

- [44] Naman D Singh, Francesco Croce, and Matthias Hein. Revisiting adversarial training for imagenet: architectures, training and generalization across threat models. In *Proceedings of the 37th International Conference on Neural Information Processing Systems (NeurIPS)*, pages 13931–13955, 2023. 2, 6, 3
- [45] Rui Tian, Zuxuan Wu, Qi Dai, Han Hu, and Yu-Gang Jiang. Deeper insights into the robustness of vits towards common corruptions. *arXiv preprint arXiv:2204.12143*, 2022. 6, 3
- [46] Hanrui Wang, Ruoxi Sun, Cunjian Chen, Minhui Xue, Lay-Ki Soon, Shuo Wang, and Zhe Jin. Iterative window mean filter: Thwarting diffusion-based adversarial purification. *IEEE Transactions on Dependable and Secure Computing*, 2024. 1, 3, 2
- [47] Hanrui Wang, Shuo Wang, Cunjian Chen, Massimo Tistarelli, and Zhe Jin. A multi-task adversarial attack against face authentication. *ACM Transactions on Multimedia Computing, Communications, and Applications*, 20(11), 2024. 1
- [48] Qinglong Wang, Wenbo Guo, Kaixuan Zhang, Alexander G Ororbia, Xinyu Xing, Xue Liu, and C Lee Giles. Adversary resistant deep neural networks with an application to malware detection. In *Proceedings of the 23rd ACM Sigkdd International Conference on Knowledge Discovery and Data Mining (ACM SIGKDD)*, pages 1145–1153, 2017. 3, 1
- [49] Zhou Wang, Alan C Bovik, Hamid R Sheikh, and Eero P Simoncelli. Image quality assessment: from error visibility to structural similarity. *IEEE Transactions on Image Processing*, 13(4):600–612, 2004. 6
- [50] Zekai Wang, Tianyu Pang, Chao Du, Min Lin, Weiwei Liu, and Shuicheng Yan. Better diffusion models further improve adversarial training. In *International Conference on Machine Learning (ICML)*, pages 36246–36263. PMLR, 2023. 2, 1, 6
- [51] Eric Wong, Leslie Rice, and J Zico Kolter. Fast is better than free: Revisiting adversarial training. In *International Conference on Learning Representations (ICLR)*, 2023. 6
- [52] Yuanheng Xu, Yanchao Sun, Micah Goldblum, Tom Goldstein, and Furong Huang. Exploring and exploiting decision boundary dynamics for adversarial robustness. In *International Conference on Learning Representations (ICLR)*, 2023. 6
- [53] Fei Yin, Yong Zhang, Baoyuan Wu, Yan Feng, Jingyi Zhang, Yanbo Fan, and Yujiu Yang. Generalizable black-box adversarial attack with meta learning. *IEEE Transactions on Pattern Analysis and Machine Intelligence*, 2023. 3, 5, 7
- [54] Hongyang Zhang, Yaodong Yu, Jiantao Jiao, Eric Xing, Laurent El Ghaoui, and Michael Jordan. Theoretically principled trade-off between robustness and accuracy. In *International Conference on Machine Learning (ICML)*, pages 7472–7482. PMLR, 2019. 1, 2
- [55] Richard Zhang, Phillip Isola, Alexei A Efros, Eli Shechtman, and Oliver Wang. The unreasonable effectiveness of deep features as a perceptual metric. In *Proceedings of the IEEE Conference on Computer Vision and Pattern Recognition (CVPR)*, pages 586–595, 2018. 6
- [56] Fei Zuo and Qiang Zeng. Exploiting the sensitivity of l2 adversarial examples to erase-and-restore. In *Proceedings of*

Fast Preemption: Forward-Backward Cascade Learning for Efficient and Transferable Proactive Adversarial Defense

Supplementary Material

This supplementary material provides an in-depth discussion of individual related works (Appendix A), the algorithms underpinning the proposed adversarial defense and adaptive reversion attack (Appendix B), model architectures (Appendix D), and the experimental configurations for both attacks and defenses (Appendix C). Additionally, it details the implementation specifics (Appendix E) and presents comprehensive ablation study results Appendix F, covering aspects such as the classifier, backbone models, the Forward-Backward Cascade Learning algorithm, and the strategy of averaging multiple Fast Gradient Sign Method (FGSM) examples.

A. Related Work

Existing adversarial defenses are divided into three categories: training-time, test-time, and preemptive.

Training-time defenses produce robust deep learning models that may correctly classify adversarial examples (AEs) as their ground truth labels. The earliest mechanisms, *e.g.*, adversarial training [18], incorporated various types of AEs along with their ground-truth labels in the training dataset. Zhang *et al.* [54] proposed TRADES, which introduces a theoretically grounded approach to balance robustness and accuracy in adversarial training by incorporating a custom loss function that controls the trade-off between clean accuracy and adversarial robustness. To improve the efficiency of training on large-scale datasets, Shafahi *et al.* [42] devised accelerated adversarial training in which backward-pass computations are reused. This entails curating a large number of specific real-world samples; Sehwag *et al.* [41] circumvented this problem by using additional data from proxy distributions learned by advanced generative models for adversarial training. Goyal *et al.* [19] demonstrated that generative models trained solely on the original dataset can be leveraged to artificially increase the training dataset’s size and improve adversarial robustness against L_p -norm perturbations. Debenedetti *et al.* [13] proposed using a custom recipe of vision transformers for adversarial training in which weaker data augmentation is used with warm-up in the augmentation intensity. Inspired by denoising diffusion models [23], Wang *et al.* [50] conducted adversarial training using data generated by an elucidating diffusion model [24]. Dong *et al.* [14] introduced robust examples (REs) generated by a preemptive defense into the adversarial training and demonstrated alleviation of clean accuracy deterioration. Peng *et al.* [35] devised a robust model which follows a suite of generalizable

robust architectural design principles: (i) an optimal range for depth and width configurations; (ii) a preference for a convolutional rather than patchify stem stage, and (iii) a robust residual block design featuring squeeze and excitation blocks and nonparametric, smooth activation functions. Bartoldson *et al.* [6] developed the current state-of-the-art (SOTA) robust model by scaling laws for adversarial training to assess robustness in image classifiers, revealing that even with significant computational resources, robustness asymptotes below human-level performance due to flaws in attack formulations generating invalid data, suggesting future efforts should address both computational efficiency and image validity.

Training-time defenses have two shortcomings. First, they require vast amounts of data for training, and the data quality and diversity are crucial to robustness. Second, training-time defenses typically reduce clean accuracy in favor of robust accuracy, even the one proposed by Dong *et al.* [14], which was designed to circumvent this problem.

Test-time defenses are divided to detection and purification. Detection models are typically trained on AEs to enable the model to distinguish them from benign inputs. Among recent studies, Cohen *et al.* [9] devised a k-nearest neighbor model for ranking the most supportive training samples for any given validation example in training a detector. Zuo and Zeng [56] proposed using a binary classifier, erase-and-restore, that uses the intriguing sensitivity of L_2 -norm attacks by randomly erasing certain pixels in an L_2 -norm AE and then restoring them with an inpainting technique. Liang *et al.* [27] detected AEs by comparing the classification results of a given sample and a denoised version that was generated through adaptive noise reduction combining scalar quantization and a smoothing spatial filter. Most recently, Hickling *et al.* [22] devised a detector using explainable deep reinforcement learning for uncrewed aerial vehicle agents. However, detection of unseen attacks is challenging for all existing detectors because they are trained on AEs from known attacks [7]. Additionally, detection always introduces errors due to false classification of benign images as AEs, thus reducing clean accuracy.

In contrast, adversarial purification aims to purify AEs by eliminating or invalidating perturbations. Earlier studies used image distortion for purification. For instance, Wang *et al.* [48] distorted images by randomly nullifying pixels. Guo *et al.* [20] preprocessed inputs with a nondifferentiable transformation. Raff *et al.* [37] combined a large number of individually weak defenses into a single randomized trans-

formation to build a strong defense. Lately, more practical approaches generate benign replacements for inputs regardless of whether they are malicious. Ren *et al.* [38] trained a generative model using autoencoder technology [25]. They claimed the existence of an immune space, in which perturbations have fewer adverse effects, and they inactivated adversarial perturbations by restricting them to that subspace. Nie *et al.* [34] devised the DiffPure benchmark, which uses denoising diffusion models [23]. DiffPure replaces perturbations with Gaussian noise and then restores the clean image by reversing the diffusion process. The major limitation of purification is that the difference between the original and generated examples degrades clean accuracy, and the possibility of being counterattacked [46].

Lastly, Alfara *et al.* [3] introduced a test-time defense mechanism incorporating preemptive defense as an anti-adversary layer guided by the output of a standard classifier. However, this defense can be circumvented if the classifier is compromised, a limitation explicitly acknowledged in their paper. This significant vulnerability undermines the practicality of using preemptive defense techniques in test-time scenarios. While they characterize this scenario as a “least realistic setting,” we contend that it aligns with the standard white-box attack paradigm, where adversaries have full access to the model. Under even more challenging assumptions, adversaries might also be aware of the defense mechanism itself (white-box reversion). Furthermore, the approach of Alfara *et al.* [3] depends exclusively on forward propagation-based learning, which increases the risk of overfitting.

Preemptive defenses aim to generate REs that replace original images, which are then discarded. These REs are more challenging to manipulate and thus resist adversarial attacks. Salman *et al.* [40] was the first to devise a preemptive defense strategy utilizing REs, which they referred to as “unadversarial” examples. They were learned using projected gradient descent (PGD) [31] and improved both in-distribution performance and robustness against unforeseen perturbations. Moon *et al.* [32] devised a Bi-Level optimization algorithm (abbreviated as Bi-Level in this paper) that finds points in the vicinity of natural images that are robust against adversarial perturbations; it achieved SOTA robust accuracy. However, its time cost is huge, and its transferability is low. Frosio and Kautz [17] introduced the A^5 (“Adversarial Augmentation Against Adversarial Attacks”) framework that uses an individual classifier and a robustifier (a generator), which are co-trained. It is much more efficient than the Bi-Level optimization algorithm, but it is not as robust.

Algorithm 1 Fast Preemption

Input: Original image x , classifier f_c , backbone model f_b , maximum L_∞ -norm distance ϵ , learning rate η , maximum forward steps T_\rightarrow and backward steps T_\leftarrow , number of examples for averaging perturbations N .

Output: Robust example x^r .

```

1: // Forward Propagation
2:  $x_0 = x$ 
3: for  $t < T_\rightarrow$  do
4:   for  $n = 1, \dots, N$  do
5:      $\delta_n \sim U(-\epsilon, +\epsilon)$   $\triangleright$  random initialization
6:      $x_{t,n} = x_t + \delta_n$ 
7:      $x_{t,n}^r = \prod_{x,\epsilon} (x_{t,n} - \epsilon \cdot \text{sign}(\nabla \ell(x_{t,n}|x, f_c, f_b)))$ 
8:      $\triangleright$  FGSM decreases  $\ell$ 
9:   end for
10:   $\delta_t^r = \frac{1}{N} \sum_{n=1}^N x_{t,n}^r - x_t$   $\triangleright$  averages perturbations
11:   $x_{t+1} = x_t + \eta \cdot \delta_t^r$   $\triangleright$  direct enhancement
12: end for
13: // Backward Propagation
14:  $x_0 = x_{T_\rightarrow}$ 
15: for  $t < T_\leftarrow$  do
16:   for  $n = 1, \dots, N$  do
17:      $\delta_n \sim U(-\epsilon, +\epsilon)$   $\triangleright$  random initialization
18:      $x_{t,n} = x_t + \delta_n$ 
19:      $x_{t,n}^a = \prod_{x,\epsilon} (x_{t,n} + \epsilon \cdot \text{sign}(\nabla \ell(x_{t,n}|x, f_c, f_b)))$ 
20:      $\triangleright$  FGSM increases  $\ell$ 
21:   end for
22:   $\delta_t^a = \frac{1}{N} \sum_{n=1}^N x_{t,n}^a - x_t$   $\triangleright$  averages perturbations
23:   $x_{t+1} = x_t - \eta \cdot \delta_t^a$   $\triangleright$  reverses the attack
24: end for
25: return  $x^r = x_{T_\leftarrow}$ 

```

Algorithm 2 Preemptive Reversion

Input: Robust example x^r .

Output: Reversed example \tilde{x} .

```

1:  $(x^r)^r = \text{PreemptiveDefense}(x^r)$   $\triangleright$  secondary defense
2:  $\tilde{x} = x^r - ((x^r)^r - x^r)$   $\triangleright$  reverses the secondary defense
3: return  $\tilde{x}$ 

```

B. Algorithms of Fast Preemption and Preemptive Reversion

The complete defense algorithm of Fast Preemption is presented in Algorithm 1. With PyTorch implementation, Steps 4 to 8 and Steps 15 to 19 can be respectively processed in parallel. The complete adaptive attack algorithm of Preemptive Reversion is presented in Algorithm 2.

Table 3. Experiment Settings.

Type	Approach	Settings
Adversarial Attack	PGD [31]	$L_\infty \epsilon = \frac{8}{255} / \frac{4}{255}^2$ or $L_2 \epsilon = 0.5^1 / 2^2$
	AutoAttack [11]	
	CW [7]	
	DeCoW [28]	
	MCG [53]	Maximum Queries = 20,000
Reversion Attack	JPEG	Quality Factor = 50%
	DiffPure [34]	Diffusion Timestep = $0.1^1 / 0.15^2$
	Fast Preemption (ours)	Same with our defense
Defense	DiffPure [34]	Diffusion Timestep = $0.1^1 / 0.15^2$
	Bi-Level [32]	$L_\infty \epsilon = \frac{8}{255} / \frac{4}{255}^2, \eta^3 = 0.1, T_{\leftarrow} = 100, N = 1$
	A^5 [17]	$L_\infty \epsilon = \frac{8}{255} / \frac{4}{255}^2$
	Fast Preemption (ours)	$L_\infty \epsilon = \frac{8}{255} / \frac{4}{255}^2, \eta^3 = 0.7, T_{\rightarrow} = 1, T_{\leftarrow} = 2, N = 20$

¹ for CIFAR-10; ² for ImageNet.

³ η must meet $\eta \cdot (T_{\rightarrow} + T_{\leftarrow}) > 1$.

Table 4. Model architectures.

Dataset	Architecture
CIFAR-10	WideResNet-94-16 [6]
	RaWideResNet-70-16 [35]
	WideResNet-34-20 [32]
	XCiT-L12 [13]
	PreActResNet-18 [19] (backbone) ResNeXt29-32x4d [21] (classifier)
ImageNet	Swin-L [29]
	ConvNeXt-L+ConvStem [44] (backbone)
	DeiT Base [45] (classifier)

C. Experiment Settings

The full experimental settings used for evaluations are listed in Tab. 3.

D. Model Architectures

We evaluated attacks and defenses using models with various architectures, as listed in Tab. 4.

E. Implementation

Our implementation partially leveraged the ART [33] and RobustBench [12] leaderboards by using PyTorch. The experimental machine was equipped with an NVIDIA A100 40GB GPU.

F. Ablation Studies

We conducted ablation studies on the Fast Preemption framework and learning algorithm using the CIFAR-10 dataset. The attacks were PGD [31] and AutoAttack (Standard) [11] with L_∞ -norm perturbations and $\epsilon = 8/255$. As illustrated in Fig. 6 of Sec. 7, Fast Preemption with the proposed framework and learning algorithm outperformed the

SOTA benchmark Bi-Level [32] in terms of clean and robust accuracies and time cost. These studies and results were aimed at identifying the optimal strategies.

F.1. Classifier

In all proactive defenses, correct labeling guarantees that optimization moves in the correct direction. As demonstrated in Tab. 5, a classifier with higher accuracy leads to better performance. As this classifier is not involved in the Fore-Back learning, the time cost of labeling inputs can be ignored compared with that of Fore-Back learning. Note that the use of ground truths is ideal, but this requires manual labeling, which is impractical for efficient user interaction. Therefore, we used the best pretrained classifier in the Fast Preemption framework, one that differs from the backbone model.

F.2. Backbone Model

The backbone model determines the defense time cost and performance. As illustrated in Fig. 7, different backbone models learn different features. To evaluate the effect of the backbone model, we also evaluated white-box defenses, for which the backbone model is the same as the victim model, *i.e.*, paired modules, as stated in Sec. 1, although we believe that this setting is not secure due to potential privacy leakage due to the existence of a backdoor [39].

As shown in Tab. 6, the best adversarially trained model was WideResNet-94-16 [6], so it is not surprising that its white-box defense outperformed that of the other backbone models. However, this most robust model failed to guarantee the best transferability (see results against XCiT-L12 [13]), and the time cost was much higher due to its complexity. We thus empirically selected PreActResNet-18 [19] as the backbone model in Fast Preemption as it had the least time cost and comparable transferability compared

Table 5. Performance with different classifiers.

Classifier	Ablation		Time Cost(s)	Transferable Defense		
	Accuracy(%)			Clean(%)	PGD(%)	AutoAttack(%)
Ground Truths	100		28	97.2	86.9	83.1
ResNeXt	95.9		28	95.4	85.7	82.7
Bi-Level	89.1		29	91.9	83.9	81.0

To evaluate the performance of diverse classifiers in our framework, we used the same backbone model and 100 steps backward propagation as Bi-Level [32]. The transferable defenses were all evaluated using RaWideResNet-70-16 [35] as the victim model. **Bold** indicates the best performance.

Table 6. Performance of different backbone models.

	Backbone Model:			
	Bi-Level [32]	WideResNet-94-16 [6]	PreActResNet-18 [19]	
Backbone Robustness	Clean (%)	89.1	93.9	88.1
	PGD (%)	43.9	77.1	61.8
	AutoAttack (%)	42.4	74.0	58.6
	Time Cost (s) for Defense	28	69	26
White-Box Defense	Clean (%)	95.5	95.8	93.8
	PGD (%)	84.9	91.6	85.9
	AutoAttack (%)	81.8	90.2	83.3
Transferable Defense Victim: RaWideResNet-70-16 [35]	Clean (%)	95.4	95.5	95.3
	PGD (%)	85.7	89.7	87.6
	AutoAttack (%)	82.7	88.0	85.9
Transferable Defense Victim: XCiT-L12 [13]	Clean (%)	95.3	95.3	95.4
	PGD (%)	72.7	78.6	79.6
	AutoAttack (%)	70.8	75.7	77.3

To evaluate the performance of the backbone models in our framework, we followed the results from the previous section and used ResNeXt29-32x4d [21] as the classifier model, and 100 steps backward propagation as Bi-Level [32]. The transferable defenses were all evaluated using RaWideResNet-70-16 [35] and XCiT-L12 [13] as the victim models, different from the backbone models. **Bold** indicates the best performance.

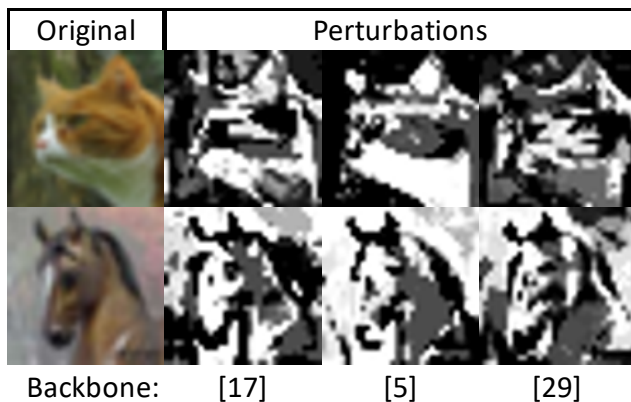


Figure 7. Different backbone models learn different features. PreActResNet-18 [19], WideResNet-94-16 [6], and Bi-Level [32] were adversarially trained, so they learned more crucial features, *i.e.*, ones that are visually similar to the objective.

with the SOTA robust model [6]. Nevertheless, it is worth investigating more comprehensive approaches for determining the backbone model in future work.

F.3. Forward-Backward Cascade Learning

As observed in Fig. 8, forward (F) propagation accelerated defense but led to overfitting (*e.g.*, F100-B0). In contrast, backward (B) propagation required more steps to converge (*e.g.*, F0-B100) but alleviated overfitting by the forward propagation (*e.g.*, F10-B90). Additionally, as shown by the curve for “Alternate,” the number of steps in forward propagation must be smaller than that in backward propagation to alleviate overfitting.

Our goal is to reduce the time cost, *i.e.*, learning steps, so we further evaluated forward and backward propagation by limiting the learning steps, as illustrated in Fig. 9. The results show that when the number of learning steps is small, the combination of forward and backward propagation outperforms backward propagation alone (*e.g.*, F1-B2 vs. F0-B3). Therefore, Fast Preemption runs one step forward and two steps backward propagation learning as the optimal strategy.

F.4. Optimization Algorithm

The results in Tab. 7 indicate that averaging N FGSM examples results in the best performance with the least time cost. Using PGD results in much more time being spent for preemptive defense, whereas using FGSM but without

Table 7. Performance for different N and optimization algorithms.

Optimization	Ablation		Time Cost (s)	Transferable Defense		
	N	Samples		Clean (%)	PGD (%)	AutoAttack (%)
PGD	1		0.7	95.3	87.5	85.8
FGSM	1		0.04	95.4	86.8	85.4
PGD	20		0.8	95.2	87.7	85.9
FGSM	20		0.04	95.5	87.8	85.9

Forward propagation ran one step and backward propagation ran two steps. Transferable defense was evaluated using RaWideResNet-70-16 [35] as the victim model. **Bold** indicates the best performance.

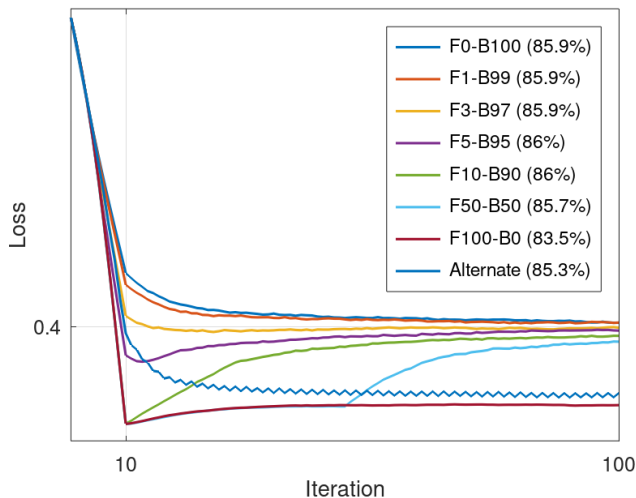


Figure 8. Forward propagation (F) converges faster while backward propagation (B) alleviates overfitting. The numbers following F and B denote the number of learning steps T_{\rightarrow} and T_{\leftarrow} , respectively. The numbers in brackets represent robust accuracy against AutoAttack (Standard). “Alternate” represents the running of forward and backward propagation alternatively for 100 steps in total.

averaging leads to poor performance.

G. Evaluation across More Models

In the main paper, we concentrated on comparisons with top-performing adversarial training methods [6, 29]. In this section, we extend our evaluation to include defenses tested across nine additional victim models on CIFAR-10 [26] from RobustBench [12] in a transferable context. These models encompass diverse architectures representative of platforms such as Twitter and Facebook, differing from both the classifier [21] and the backbone model [19].

As shown in Tab. 8, our method demonstrates significant performance gains compared to no proactive defense and the SOTA proactive defense [32]. Specifically, we achieve average improvements of 4.2% and 4.3% in clean accuracy, 17.8% and 5% in robust accuracy, and a 700-fold in-

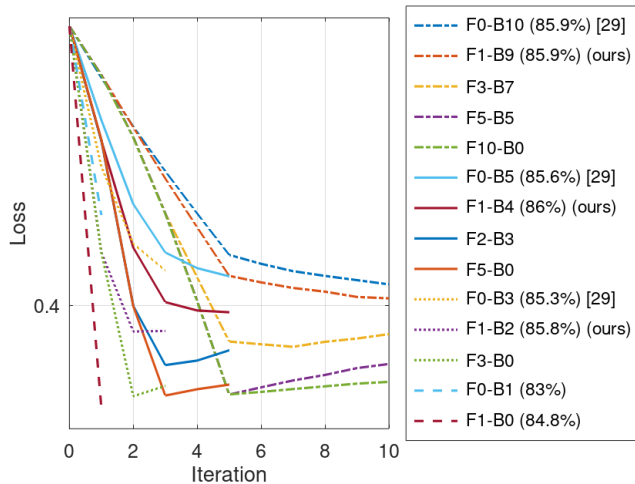


Figure 9. By combining forward (F) and backward (B) propagation, Fast Preemption obtains performance comparable to that of the SOTA preemptive defense [32] by using only three steps (F1–B2). The numbers following F and B denote the number of learning steps T_{\rightarrow} and T_{\leftarrow} , respectively. The numbers in brackets represent robust accuracy against AutoAttack (Standard).

crease in speed, respectively. Furthermore, compared using the SOTA adversarial training model [6] as the backbone model, our chosen [19] yields an average increase of 0.7% in clean accuracy, 2.5% in robust accuracy, and a tenfold improvement in processing speed.

H. Defense against More Attacks

Our primary evaluation adheres to the RobustBench [12] protocol, employing the strongest attack, AutoAttack [11]. As detailed in Sec. 5.2, this includes tests with standard and randomized AutoAttack variants, encompassing white-box APGD [11], FAB [10], and black-box Square [4] attacks, alongside EOT settings [5].

In this section, we extend the evaluation to include three additional attacks: white-box Carlini-Wagner (CW) [7], black-box Deformation-Constrained Warping (DeCoW) [28], and black-box Meta Conditional Generator (MCG) [53], demonstrating the broad applicability and gen-

Table 8. Transferable clean and robust accuracy (%) across various victim models against AutoAttack (Standard) [11] with L_∞ -norm perturbations and $\epsilon = 8/255$. All proactive defenses were conducted using classifier and backbone models distinct from the victim models, even when the architectures were similar.

Model	Metric	No Proactive Defense	Bi-Level [32]	Fast Preemption (ours)	
Defense Learning	Backbone Time Cost (s)	N/A N/A	Bi-Level [32] 28	WideResNet-94-16 [6] 0.35	PreActResNet-18 [19] 0.04
RaWideResNet-70-16 [35]	Clean	93.5	92.1	95.5	95.4
	Robust	71.4	81.3	86.8	85.9
WideResNet-70-16 [50]	Clean	93.3	91.5	95.5	95.3
	Robust	71.2	80.9	86.4	86.0
WideResNet-34-10 [36]	Clean	91.5	90.2	95.1	95.1
	Robust	62.1	76.2	78.7	80.8
WideResNet-28-10 [52]	Clean	93.4	91.5	95.4	95.6
	Robust	64.8	77.7	81.3	83.2
PreActResNet-18 [51]	Clean	84.2	87.3	90.1	91.6
	Robust	42.4	54.7	55.4	61.2
ResNest152 [41]	Clean	86.9	87.6	91.2	92.4
	Robust	62.4	73.2	75.8	78.2
ResNet-50 [8]	Clean	86.6	88.5	91.6	93.2
	Robust	52.0	68.1	66.7	72.0
ResNet-18 [1]	Clean	86.6	88.1	91.5	92.7
	Robust	51.4	67.5	67.8	72.8
XCiT-L12 [13]	Clean	92.8	91.2	95.1	95.4
	Robust	57.9	71.3	74.6	76.0
Average	Clean	89.9	89.8	93.4	94.1
	Robust	59.5	72.3	74.8	77.3

Bold indicates the best performance.

eralizability of our defense against diverse attack strategies.

As shown in Tab. 9, our defense achieves robust accuracy of 90.3%, 93.6%, and 87.3% against CW, DeCoW, and MCG attacks, respectively, outperforming SOTA adversarial training [6] and proactive defenses [32]. Notably, these accuracies exceed those obtained against AutoAttack, further highlighting the robustness and reliability of our primary evaluation.

I. Visual Quality

The noise budgets utilized (as detailed in Tab. 3) adhere to standard practices in adversarial machine learning, ensuring the preservation of visual quality and minimizing the likelihood of detection. As illustrated in Fig. 10, for 1,000 images from CIFAR-10 and ImageNet, Structural Similarity Index Measure (SSIM) [49] and Learned Perceptual Image Patch Similarity (LPIPS) [55] scores confirm that the visual quality of our robust examples (REs) is sufficiently high to serve as effective substitutes for the original images. Furthermore, our REs exhibit comparable (often superior) visual quality relative to adversarial examples (AEs) and outputs of existing defense methods.

I.1. Structural Similarity Index (SSIM)

The SSIM is a metric for measuring similarity between two images. It considers luminance, contrast, and structural information. The SSIM between two images x (reference) and y (distorted) is defined as:

$$SSIM(x, y) = \frac{(2\mu_x\mu_y + C_1)(2\sigma_{xy} + C_2)}{(\mu_x^2 + \mu_y^2 + C_1)(\sigma_x^2 + \sigma_y^2 + C_2)}, \quad (15)$$

where:

- μ_x and μ_y : Mean intensity values of x and y , respectively.
- σ_x^2 and σ_y^2 : Variance of x and y , respectively.
- σ_{xy} : Covariance between x and y .
- C_1 and C_2 : Small constants added to stabilize the metric in the presence of weak denominators, defined as:

$$C_1 = (K_1L)^2, \quad C_2 = (K_2L)^2, \quad (16)$$

where L is the dynamic range of the pixel values (e.g., 255 for 8-bit images), and K_1 and K_2 are small positive constants (commonly, $K_1 = 0.01$ and $K_2 = 0.03$).

The SSIM value ranges from -1 to 1, where:

- 1: Perfect similarity.
- 0: No similarity.
- Negative values indicate dissimilarity.

SSIM is typically calculated locally using a sliding window across the image, and the overall SSIM is the average of local SSIM values. Higher SSIM values denote subtler deviations from the reference images.

Table 9. Robust accuracy (%) against various adversarial attacks with L_∞ -norm perturbations and $\epsilon = 8/255$.

Threat Model	Attack	WideResNet-94-16 [6]	Bi-Level [32]	Fast Preemption (ours)
White-Box	AutoAttack (Standard) [11]	74.0	82.1	86.3
	CW [7]	80.8	85.4	90.3
Black-Box	DeCoW [28]	88.8	89.7	93.6
	MCG [53]	76.1	83.3	87.3

Bold indicates the best performance.

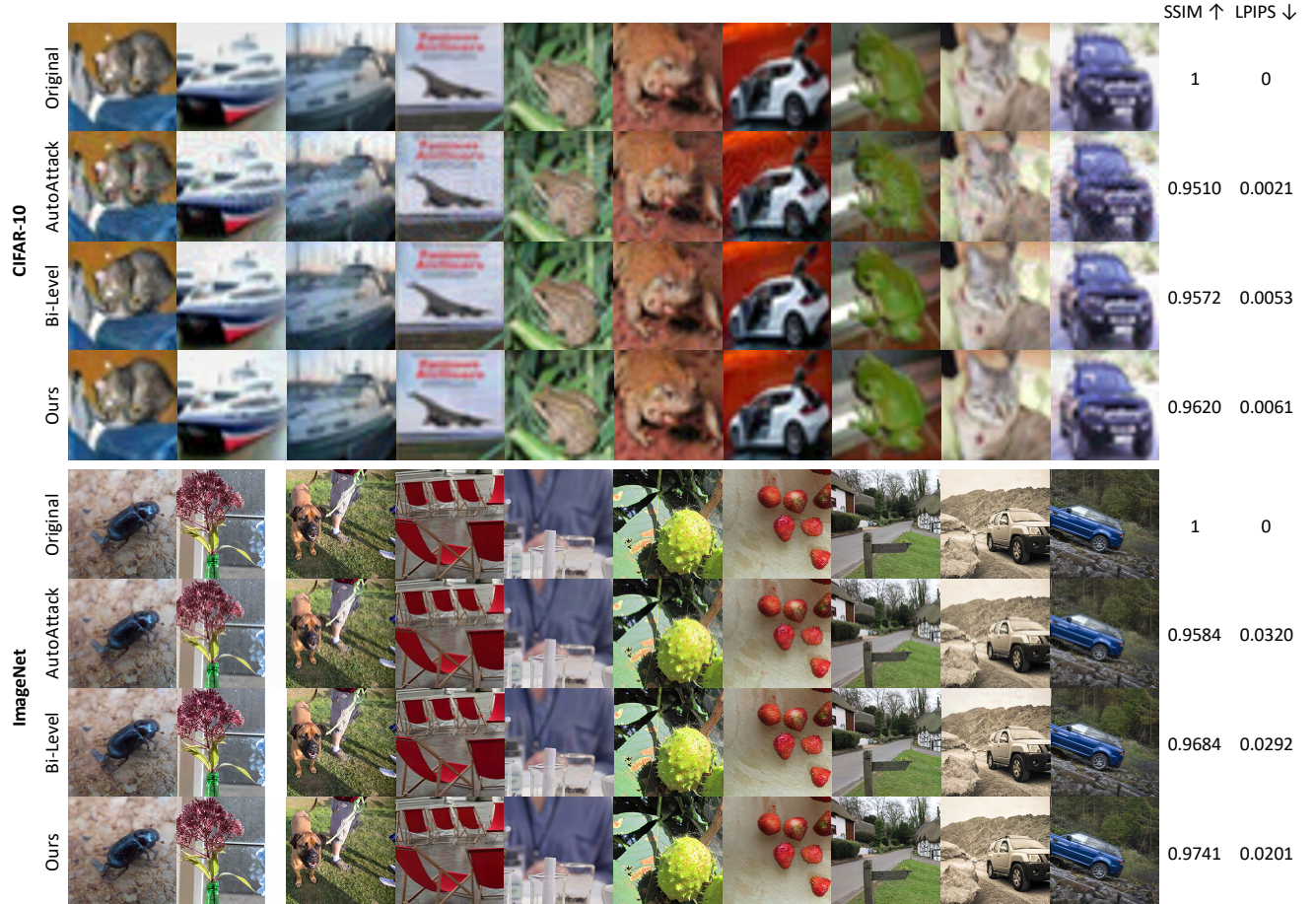


Figure 10. Visual quality of robust examples (REs) generated by our Fast Preemptive defense, compared with adversarial examples (AEs) from AutoAttack and REs from the SOTA proactive defense [32]. All samples adhere to the same L_∞ -norm constraint ($\epsilon = 8/255$) relative to the original images. SSIM and LPIPS scores demonstrate that the visual quality of our REs is sufficiently high to serve as replacements for the original images, and is comparable to (and often slightly better than) those of the adversarial attack and existing defense methods.

I.2. Learned Perceptual Image Patch Similarity (LPIPS)

The LPIPS is a perceptual similarity measure that evaluates the perceptual distance between two images. It uses deep neural network features to compare the visual content and correlates better with human perception than traditional metrics like SSIM.

The LPIPS distance between two images x (reference) and y (distorted) is computed as:

$$LPIPS(x, y) = \sum_l \frac{1}{H_l W_l} \sum_{h=1}^{H_l} \sum_{w=1}^{W_l} w_l \|\hat{\phi}_l(x)_{h,w} - \hat{\phi}_l(y)_{h,w}\|_2^2, \quad (17)$$

where:

- l : Layer index in the deep network.
- $\phi_l(x)$: Feature map of x at layer l in the network.

- $\hat{\phi}_l$: Normalized feature maps for each channel.
- H_l, W_l : Height and width of the feature map at layer l .
- w_l : Learned scalar weights for each layer l (trained to match human judgments).

LPIPS uses a pretrained deep neural network to extract feature maps from intermediate layers. The metric normalizes the feature maps and computes the difference between them, weighted according to the learned weights w_l . The LPIPS value typically ranges from 0 (perfect perceptual similarity) to higher values indicating greater dissimilarity. LPIPS provides a perceptually grounded comparison, making it especially useful for evaluating subtle changes in visual quality.